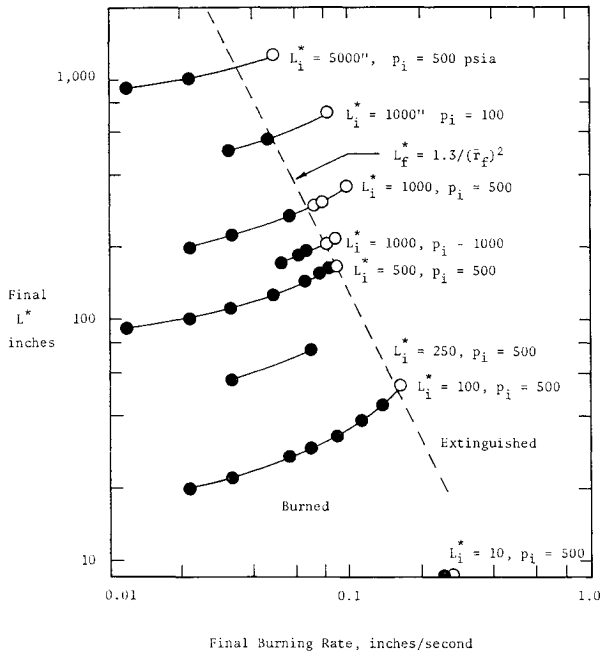

Fig. 5 Correlation of predicted termination transients; the data are plotted without regard for variations in dp/dt.

(Fig. 1) show that the marginal $(dp/dt)_i$ increases as p_i increases, in accordance with customary experimental observations.

In the second set of calculations L_i^* was varied from 100 in. to 5000 in. for p_i = 500 psia (K_n = 186.3) and an opening time of 0.2 msec. The marginal $(dp/dt)_i$ was predicted to be reduced from 70,000 psi/sec to less than 10,000 psi/sec as L^* was increased from 100 in. to 5000 in. (Fig. 2). Experimental data extracted from Ref. 8 show this same trend (Fig. 2).

In the next set of calculations the nozzle opening time was increased to 20 msec; the surprising result was that the marginal over all nozzle-area change was affected very little (Fig. 3). Figure 4 shows that the predicted effect of the greater opening time is to decrease dp/dt by approximately a factor of four until p reaches 100 psia. At this p, which corresponds to a time just prior to the nozzle being completely open, the $d(\ln p)/dt$ for the slowly opened case suddenly increases to near that of the rapidly opened case. This rapid change is apparently due to transient burning rate effects. For both cases illustrated, the nozzle-area ratio is near the marginal ratio below which extinguishment does not occur. Thus the important point illustrated by this figure is that the initial depressurization rate does not distinguish marginal extinguishment conditions in this case and, therefore, appears to have little value to the designer.

After several attempts using different approaches, it was discovered that all of the results of this parametric study could be correlated in terms of the motor L^* following opening of the nozzle L^*_f, and the burning rate $\bar{r}_f$ that would result from the nozzle-area change provided steady-state ballistics apply. Figure 5 presents all of the data plotted this way. The line $L^*_f = 1.3/\bar{r}^2$ provides a reasonable correlation of the marginal extinguishment conditions.

References

[1] Horton, M. D., Bruno, P. S., and Graesser, E. C., "Depressurization Induced Extinction of Burning Solid Propellants," *AIAA Journal*, Vol. 6, No. 2, Feb. 1968, pp. 292–297.

[2] Wooldridge, C. E., Marximan, G. A., and Kier, R. J., "A Theoretical and Experimental Study of Propellant Combustion Phenomena during Rapid Depressurization," Final Report, Contract NAS 1-7349, Feb. 1969, Stanford Research Institute, Menlo Park, Calif.

[3] Merkle, C. L., Turk, S. L., and Summerfield, M., "Extinguishment of Solid Propellants by Rapid Depressurization: Effects of Propellant Parameters," AIAA Paper 69-176, New York, 1969.

[4] Coates, R. L. and Horton, M. D., "Prediction of Conditions Leading to Extinguishment," *Proceedings of 6th ICRPG Combustion Conference*, CPIA Publications 192, Vol. 1, Dec. 1969, Silver Spring, Md., pp. 399–409.

[5] Ciepluch, C. C., "Effect of Rapid Pressure Decay on Solid Propellant Combustion," *ARS Journal*, Vol. 31, 1961, pp. 1584–1586.

[6] Ciepluch, C. C., "Effect of Composition on Combustion of Solid Propellants Using a Rapid Pressure Decrease," TN D-1559, 1962, NASA.

[7] "A Stop Start Study of Solid Propellants," Final Report, Contract NAS 1-6601, Nov. 1967, United Technology Center, Sunnyvale, Calif.

[8] "An Experimental Study of Solid Propellant Extinguishment by Rapid Depressurization," Preliminary Final Report, Contract NAS 1-7815, 1969, United Technology Center, Sunnyvale, Calif.

[9] Denison, M. R., and Baum, E., "A Simplified Model of Unstable Burning in Solid Propellants," *ARS Journal*, Vol. 31, No. 8, Aug. 1961, pp. 1112–1122.

[10] Coates, R. L., Polzien, R. E., and Price, C. F., "Design Procedures for Combustion Termination by Nozzle Area Variation," *Journal of Spacecraft and Rockets*, Vol. 3, No. 3, March 1966, pp. 418–425.

[11] Conte, S. D., *Elementary Numerical Analysis*, McGraw-Hill, New York, 1965, pp. 234–238.

Dynamic Response of Hydraulic Hoses

G. M. SWISHER*
Wright State University, Dayton, Ohio
AND
E. O. DOEBELIN†
Ohio State University, Columbus, Ohio

THE effects of hydraulic line dynamics on the over-all performance of a hydraulic control system were reported earlier.[1] Distributed-parameter and lumped-parameter models of metal lines were compared. This Note addresses the effects when braided hydraulic hoses, which expand when pressurized, are used. No investigators have reported on the degrading effect on dynamic response that occurs when hydraulic hoses are used in control systems.

The system studied was a closed-loop electrohydraulic position servo consisting of 1) a hydraulic cylinder as the power device; 2) two linear variable differential transformers (LVDT's) as the feedback and measurement elements; 3) an electronic servoamplifier with a summing circuit for comparing voltages representing the actual and desired positions of the cylinder; 4) a servovalve driven by an electromagnetic torque motor; 5) hydraulic hoses connecting the ports of the cylinder with the ports of the servovalve; 6) a full-wave-phase, sensitive demodulator which receives the measurement LVDT signal; and 7) a frequency response analyzer which provides the sinusoidal test signal and analyzes the return signal to give frequency response data.

Three models of the fluid lines were compared with the experimental results. The dynamic response was defined in terms of the actual and desired positions of the piston. The simplest line model is obtained by assuming that the pressures and flows remain uniform all along the line. This

Received September 21, 1970.

* Assistant Professor of Engineering.
† Professor of Mechanical Engineering.

neglects fluid inertia and friction. The effect of fluid compressibility in the line is accounted for by including the volume of fluid in the line with the piston enclosed volume. This is referred to as the no-inertia line model.

Another assumption in common use today is that the fluid line can be represented by several "lumps." Each lump may have compliance, friction, and inertia as desired. The number of lumps necessary for results that compare favorably with the distributed parameter results is a reasonable question to ask. Experience has shown that a good rule of thumb for steel lines is to select the number of lumps such that there are ten lumps per wavelength at the highest frequency of interest. Here it is necessary to have some estimate of the frequency spectrum of the expected input signals. "Wavelength" λ refers to the wavelength of signal propagation in a continuous fluid medium and is governed by the usual law for systems governed by the wave equation, namely

$$\lambda \triangleq \text{velocity of propagation/frequency} \tag{1}$$

The pressures and velocities are assumed to be uniform for each lump of fluid. Newton's law for a lump of fluid gives:

$$P_{n-1} - P_n = \rho_0 \text{ as } v_n \tag{2}$$

where P_{n-1} and P_n are Laplace transforms of pressure at lumps $n-1$ and n, respectively; ρ_0 is the mass density of the fluid; a is the lump length; s is the Laplace variable, and v_n is the Laplace transform of velocity of lump n.

For a short time dt, conservation of mass for the nth lump, gives:

$$v_{n-1} - v_n = aK_L s P_n \tag{3}$$

where K_L is the combined line and fluid compliance. These two equations give the desired number of equations for the number of lumps necessary to have 10 lumps per wavelength.

The third type of analysis considers the distributed-parameter nature of the fluid lines. The equations obtained here, in general, are the water-hammer partial differential equations. They are derived in Ref. 2 and are shown here in the Laplace transformed state:

$$\cosh\beta_1 P(O,s) - z_0 \sinh\beta_1 v(O,s) = P(L,s) \tag{4}$$

$$-1/z_0 \sinh\beta_1 P(O,s) + \cosh\beta_1 v(O,s) = v(L,s) \tag{5}$$

where $P(O,s)$ and $v(O,s)$ are Laplace transforms of pressure and velocity, respectively, at any station; $P(L,s)$ and $v(L,s)$ are Laplace transforms of pressure and velocity at distance L down the line; z_0 is the characteristic hydraulic impedance of line; and β_1 is the characteristic function of Laplace variable s.

If one examines a small section of hydraulic hose, one might expect a result which is similar to a metal line result. When compared to metal piping or to rigid tubing, hose expands considerably when pressurized. This expansion can lead to a "sponginess" when the system is subjected to a disturbance input. A system using hose very nearly acts as if it had an oil of low bulk modulus. Most manufacturers have static volumetric expansion data on their hoses. A typical curve is that of the Aeroquip Corporation hose 1503-4 in. shown in Fig. 1. In terms of the combined static compliance K_L, the hose-fluid combination effect is due almost completely to the hose expansion rather than the fluid bulk modulus effect. In contrast, the metal tubing-fluid compliance K_C is mainly due to the fluid bulk modulus effect. Figure 1 is very nearly linear with pressure, especially if the system is operating at some fairly high equilibrium pressure, say 1000 psi. This assumption of linearity about some operating pressure point allows the calculation of K_L from

$$V = \bar{V}(1 + K_L P_P) \tag{6}$$

where V and $\bar{V}$ are the volume of fluid and the mean volume of fluid, respectively, and P_P is the pressure difference between the actual line pressure and the equilibrium operating point pressure. The use of K_L as a measure for dynamic response of hoses is investigated. The actual hoses tested were Aeroquip 1503-4 type with 0.188-in. i.d. and 0.516-in. o.d. They had a synthetic rubber inner tube, cotton inner braid, single-wire-braid reinforcement, and cotton braid cover. The recommended hose working pressure was 3000 psi with a minimum burst pressure of 12,000 psi.

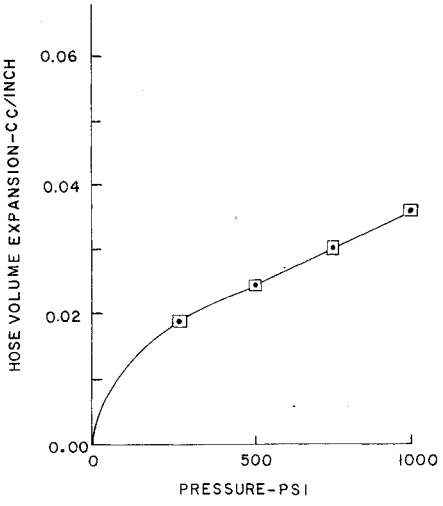

Fig. 1 Hose volumetric expansion vs. applied internal pressure.

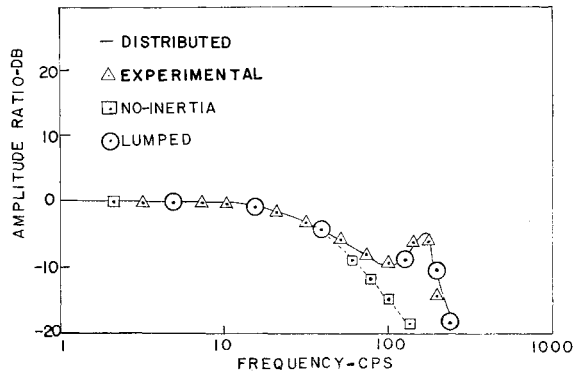

Fig. 2 Frequency responses of output motion vs desired piston motion for various hose line models.

All three types of analyses lead to tedious algebra in order to obtain the frequency response between the output piston motion and the input voltage. In the case of the no-inertia model, there were 5 simultaneous equations. The 10-lump-per-wavelength model required 13 equations and the distributed parameter model required 9 equations. The procedure adopted was the numerical solution by an IBM-360 digital computer at each frequency.

For the experimental test, 1) input sine wave frequency was limited to the range of 1 to 1000 cps and 2) input sine wave amplitude was 4.0v peak to peak (this corresponded to a piston motion of 0.020 in. peak to peak). For the comparison in Fig. 2, only the amplitude ratio is shown for the transfer function relating the input voltage to the output piston position. The distributed-parameter and the 10-lump-per-wavelength models agree very well with the experimental results for all frequencies. The validity of the no-inertia assumption breaks down at about 30 cps. For short lengths of hose (2 lumps or less), the use of K_L and the lumped model are recommended for system design purposes. With increasing number of lumps, the complex algebra involved in solving for the frequency response nullifies the advantage of simplicity that the lumped-parameter model has. In addition, the 10-lump-per-wavelength model took 4 times more computer time than the distributed parameter model when a matrix

inversion technique was used to solve for the frequency responses.[2]

References

[1] Swisher, G. M. and Doebelin, E. O., "Lumped-Parameter Modeling vs Distributed Parameter Modeling for Fluid Control Lines," *Journal of Spacecraft and Rockets*, Vol. 7, No. 6, June 1970, pp. 766–767.

[2] Swisher, G. M., "A Theoretical and Experimental Investigation of the Dynamics of Hydraulic Control Systems Connected by Long Lines or Hoses," Ph.D. dissertation, 1969, The Ohio State Univ., Columbus, Ohio.

Predicted Coolant Heat Transfer and Friction Compared with Nuclear Rocket Test Results

MAYNARD F. TAYLOR*
NASA Lewis Research Center, Cleveland, Ohio

Nomenclature

A = cross-sectional area
C_g = coefficient in heat-transfer equation
c_1 = exponent of T_w/T_b, Eq. (1)
D = diameter
e = relative roughness of surface
F = entrance effect coefficient
f = friction coefficient
G = weight flow rate per unit cross-sectional area
g = gravitational conversion factor
Nu = Nusselt number
Pr = Prandtl number
Δp = total static pressure drop
Δp_{fr} = friction pressure drop
Δp_{mom} = momentum pressure drop
R = radius of curvature
Re = Reynolds number
r = inside radius of passage
S = surface area
T = temperature
w = weight flow rate
x = linear distance from entrance
ρ = density

Subscripts

C,M = calculated and measured, respectively
b,c = bulk and crown, respectively
g,w = gas and wall, respectively
s = straight tube or reference value

Introduction

AN equation based on all available heat-transfer data for single-phase hydrogen flow through straight tubes was shown earlier[1] to correlate the data for a wide range of conditions including heat fluxes up to 27.6 Btu/sec/in.[2] (Ref. 2). The equation also was modified to include the effects of curvature[3] and compared with experimental data for single curved tubes.[2,4] The results and recommended applications of the equations have been reported.[5] Another equation[6] based on all available friction coefficient data for straight tubes was modified to include the effects of curvature.[3] In this Note these correlation equations are brought together and used to revise the coolant side calculations in an existing digital computer program for design and evaluation of convectively cooled rocket nozzles.[7] Gas-side wall temperature, coolant pressure drop, and coolant temperature rise predicted by this revised code are compared with measured values from several NERVA nuclear tests. Wall temperatures were not measured in Phoebus 2 and Pewee nuclear tests, so that only measured coolant temperature rise and pressure drop are compared with predictions. It should be noted that, although Pewee, NERVA, and Phoebus 2 vary a great deal in size and power, their nozzles have similar geometry; these calculation procedures should be compared with experiments for other geometries when available.

Presented as Paper 70-661 at the AIAA 6th Propulsion Joint Specialist Conference, San Diego, Calif., June 15–19, 1970; submitted July 6, 1970; revision received September 2, 1970.

* Nuclear Engineer.

Basic Equations

Coolant side

Heat-transfer coefficients in the coolant passages are calculated using the straight-tube correlation equation[1]

$$Nu_{b_s} = 0.023 Re_b^{0.8} Pr_b^{0.4} (T_w/T_b)^{-c_1} \quad (1)$$

where $c_1 = 0.57 - 1.59\,D/x$, and modifying it[5]

$$Nu_b = Nu_{b_s}(1 + F_1 D/x) \quad (2)$$

where $F = 2.3$ for a 45° angle bend and 5 for a 90° angle bend.

The Itō correction for the effects of curvature on friction coefficients[3] has been applied to local heat-transfer coefficients with good results[5] using Eq. (1) to give

$$Nu_b = Nu_{b_s}[Re_b(r/R)^2]^n \quad (3)$$

where

$$n = 0.05 \text{ for the concave side (throat)} \quad (3a)$$

$$n = -0.05 \text{ for the convex side (knuckle)} \quad (3b)$$

Equations (1–3a) cover all the conditions encountered in the cooling passages of nuclear rocket nozzles.

Measured friction coefficients can be as much as three times the values predicted by conventional methods.[6] Reference 6 recommended

$$f_s/2 = (0.0007 + 0.0625/Re_w^{0.32})(T_w/T_b)^{-0.5} \quad (4)$$

For $Re_w \geq 3000$, Eq. (4) correlated all of the friction coefficients within ±10%. It can be used at x/D as low as 3 by using c_1 as the exponent of T_w/T_b. The Kármán-Nikuradse relation can also be modified with $(T_w/T_b)^{-c_1}$ to give

$$f_s = [4.0 \log(Re_w f_s^{1/2}) - 0.40]^{-2}(T_w/T_b)^{-c_1} \quad (5)$$

Assuming that the effect of T_w/T_b is the same for a rough tube as it is for a smooth tube, the equation for a rough tube[7] becomes

$$f_s = [-4.0 \log(e/3.7D + 1.255/Re_w f_s^{1/2})]^{-2}(T_w/T_b)^{-c_1} \quad (6)$$

where e is the relative roughness of the tube. The Itō correction for the effect of curvature[3] should be used with Eqs. (5) and (6) as follows:

$$f = f_s[Re_w(r/R)^2]^{0.05} \quad (7)$$

The exponent in Eq. (7) is 0.05 for both the throat and knuckle regions because, unlike the heat-transfer coefficient which is affected by only the heated surface, f is affected by the wetted surface of the coolant passage. How well the Itō correction applies to local heat transfer and friction has not been studied thoroughly due to the paucity of local experimental data.

The friction and momentum pressure drops are calculated from

$$\Delta p_{fr} = 2fG^2x/Dg \quad (8)$$

$$\Delta p_{mom} = w^2/gA[(\rho A)_2^{-1} - (\rho A)_1^{-1}] \quad (9)$$

The total pressure drop is the sum, $\Delta p_{fr} + \Delta p_{mom}$.